Available online at www.sciencedirect.com
ScienceDirect
Bioorganic & Medicinal Chemistry 15 (2007) 5620–5628
Bioorganic & Medicinal Chemistry

# Characterized mechanism of α-mangostin-induced cell death: Caspase-independent apoptosis with release of endonuclease-G from mitochondria and increased miR-143 expression in human colorectal cancer DLD-1 cells

Yoshihito Nakagawa,[a] Munekazu Iinuma,[b] Tomoki Naoe,[c] Yoshinori Nozawa[a] and Yukihiro Akao[a,*]

[a]*Gifu International Institute of Biotechnology, 1-1 Naka-Fudogaoka, Kakamigahara, Gifu 504-0838, Japan*
[b]*Gifu Pharmaceutical University, 5-6-1 Mitahora-higashi, Gifu 505-0004, Japan*
[c]*Department of Hematology, Nagoya University, Graduate School of Medicine, 65 Tsurumai-cho, Showa-ku, Nagoya 466-8550, Japan*

Received 1 March 2007; revised 27 April 2007; accepted 28 April 2007
Available online 18 May 2007

**Abstract**—α-Mangostin, a xanthone from the pericarps of mangosteen (*Garcinia mangostana* Linn.), was evaluated for in vitro cytotoxicity against human colon cancer DLD-1 cells. The number of viable cells was consistently decreased by the treatment with α-mangostin at more than 20 μM. The cytotoxic effect of 20 μM α-mangostin was found to be mainly due to apoptosis, as indicated by morphological findings. Western blotting, the results of an apoptosis inhibition assay using caspase inhibitors, and the examination of caspase activity did not demonstrate the activation of any of the caspases tested. However, endonuclease-G released from mitochondria with the decreased mitochondrial membrane potential was shown. The levels of phospho-Erk1/2 were increased in the early phase until 1 h after the start of treatment and thereafter decreased, and increased again in the late phase. On the other hand, the level of phospho-Akt was sharply reduced with the process of apoptosis after 6 h of treatment. Interestingly, the level of microRNA-143, which negatively regulates Erk5 at translation, gradually increased until 24 h following the start of treatment. We also examined the synergistic growth suppression in DLD-1 cells by the combined treatment of the cells with α-mangostin and 5-FU which is one of the most effective chemotherapeutic agents for colorectal adenocarcinoma. The co-treatment with α-mangostin and 5-FU, both at 2.5 μM, augmented growth inhibition compared with the treatment with 5 μM of α-mangostin or 5 μM 5-FU alone. These findings indicate unique mechanisms of α-mangostin-induced apoptosis and its action as an effective chemosensitizer.


## 1. Introduction

The pericarps of mangosteen, *Garcinia mangostana* Linn, have been used as traditional medicine for treatment of skin infection and wounds in Southeast Asia for many years. Based on a previous study, we reported a potent cytotoxic activity of six xanthones from the pericarps of mangosteen against human leukemia HL60 cells and among them, α-mangostin-induced mitochondrial dysfunction.[1] Moreover, we reported that α-mangostin-induced cell cycle arrest and apoptosis which was determined by morphological findings and DNA ladder formation in human colon cancer DLD-1 cells.[2]

Many serine/threonine protein kinases control cell growth, proliferation, differentiation, the cell cycle, survival, and death. Mitogen-activated protein kinases (MAPKs) and Akt are key regulatory proteins in cells. MAPKs are a widely conserved family of serine/threonine protein kinases involved in many cellular programs such as cell proliferation, differentiation, motility, and death.[3] Akt, another serine/threonine protein kinase, is associated with cell survival, growth, and glycogen metabolism.[4] Various phytochemicals, including epigallocatechin-3-gallate,[5] resveratrol,[6] arucanolide[7], etc., have been shown to modulate the signaling pathways of MAPKs and/or Akt, leading to growth inhibition

*Keywords*: α-Mangostin; Apoptosis; Endonuclease-G; miR-143; Chemosensitizer.
* Corresponding author. Tel.: +81 583 71 4646; fax: +81 583 71 4412; e-mail: yakao@giib.or.jp

0968-0896/$ - see front matter © 2007 Elsevier Ltd. All rights reserved.
doi:10.1016/j.bmc.2007.04.071

and cell death. MicroRNAs (miRNAs) are recently discovered short regulatory RNA molecules representing a new layer in post-transcriptional regulation of gene expression. Although more than 450 human miRNAs have been identified, only a very few of them have been characterized in detail. A large amount of miR-143 is expressed specifically in normal colon cells; however, its expression in human colon cancer tumors is markedly decreased.[8,9] We previously determined its target mRNA to be *ERK5* by introducing miRNA-143 into DLD-1 cells.[8]

Here, using human colon cancer DLD-1 cells we show that 20 μM α-mangostin-induced caspase-independent apoptosis mediated by endonuclease-G released from mitochondria. The signaling pathways including Erk1/2, Erk5, and Akt were demonstrated to contribute to this α-mangostin-induced apoptosis. We also discovered synergistic growth suppression of these cells by the combined treatment with α-mangostin and 5-FU at certain concentrations. These findings suggest the potential therapeutic applicability of the phytochemical α-mangostin, especially when employed with 5-FU.

## 2. Results

### 2.1. Cytotoxicity of α-mangostin in human colon cancer DLD-1 cells

We examined α-mangostin at various concentrations for its cytotoxic effect on DLD-1 cells, as judged from the results of the Trypan blue-exclusion test (Fig. 1a). The growth of DLD-1 cells was suppressed by the treatment with α-mangostin at the concentration of more than 2 μM, and the concentration for 50% inhibition (IC50) was 7.5 ± 0.3 μM. Apoptotic cell death was observed at more than 15 μM. At 20 μM, the viable cell number was consistently decreased (Fig. 1b) during the treatment; and typical apoptotic changes were observed, as indicated by morphological parameters (nuclear condensation and fragmentation) at 24 h after the start of treatment (Fig. 1c).

### 2.2. Mechanism of α-mangostin-induced apoptosis

We first examined the activation of apoptosis signal pathways induced by the treatment of the DLD-1 cells with 20 μM α-mangostin. Apoptosis has been well

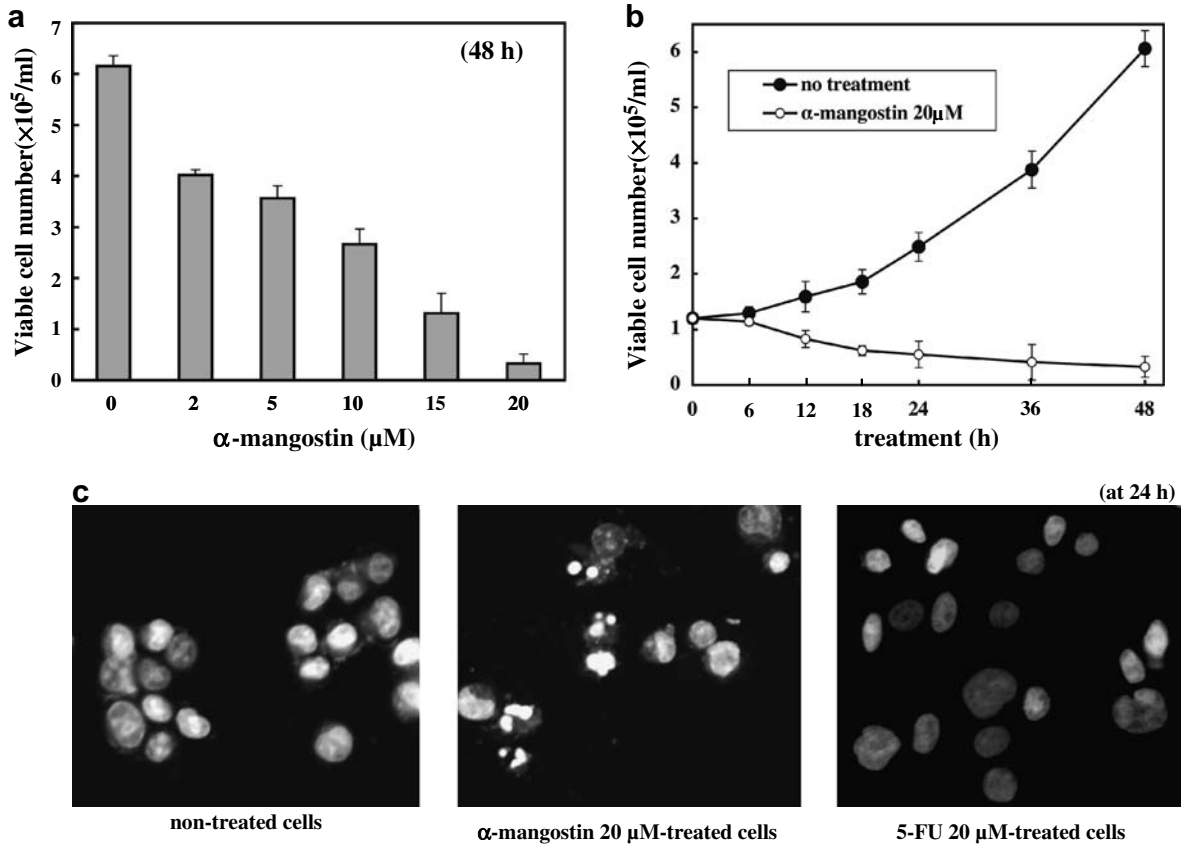


**Figure 1.** Effect of α-mangostin on growth of cells of human colon cancer cell line DLD-1. (a) Growth inhibitory effect at various concentrations of α-mangostin. Viable-cell numbers after treatment with α-mangostin were evaluated by use of the Trypan blue dye-exclusion test. (b) Growth inhibitory effect of 20 μM α-mangostin against DLD-1 cells. Viable-cell numbers after treatment with α-mangostin were evaluated by the Trypan blue dye-exclusion test. ●, no treatment; ○, 20 μM α-mangostin. (c) Morphological assessment of cell death by treatment with 20 μM α-mangostin or 5-FU. The cells were stained with Hoechst 33342 (5 μg/ml) for 30 min and then examined by fluorescence microscopy. Left panel, cells without treatment; middle, treatment with 20 μM α-mangostin for 24 h; right, 20 μM 5-FU for 24 h.

known to be executed by the cascade activation of initiator caspases (e.g., caspase-8 and -9) and executioner ones (e.g., caspase-3 and -7). To know which caspase(s) is involved in α-mangostin-induced apoptosis, we examined the formation of active forms of caspases in cell lysates by Western blot analysis. No processed active form of caspase-3 tested was observed after the treatment with 20 μM α-mangostin (Fig. 2a). In addition, pretreatment with the pan-caspase-like protease inhibitor Z-VAD-FMK or the caspase-3-specific inhibitor Z-DEVD-FMK was unable to prevent apoptosis by α-mangostin (Fig. 2b). Moreover, the activities of caspase-3 and -8 in α-mangostin (20 μM)-treated DLD-1 cells were not changed by the treatment (Fig. 2c). These results indicate that caspases were not involved in the apoptosis induced by α-mangostin.

Next we examined the mitochondrial pathway of apoptosis, which plays a crucial role in propagation and determination of cell death. The mitochondrial membrane potential evaluated by Mito-Tracker Orange was significantly perturbed at 6 h after the treatment (Fig. 2d). bcl-2 Protein present on the mitochondrial membrane inhibits the loss of mitochondrial membrane potential induced by apoptotic signals. On the other hand, the proapoptotic protein bax in the cytosol, when translocated to mitochondria, promotes the loss of mitochondrial membrane potential.[10] Western blot analysis showed that the expression of neither protein was changed in cells undergoing α-mangostin-induced apoptosis (Fig. 2a). Then we examined apoptosis-inducing factor (AIF) and endonuclease-G (Endo-G), which are two mitochondrial factors that are released from mitochondria during apoptosis. Western blot analysis showed that the level of Endo-G released following α-mangostin treatment at 20 μM was markedly increased at 6 h and sustained until 24 h (Fig. 2a), but that the amount of AIF was not changed (data not shown). The amount of Endo-G released at 6 h of α-mangostin treatment showed a dose-dependent increase (Fig. 2a).

### 2.3. Effect of α-mangostin treatment on MAP and Akt kinases

When we examined the activation of MAP kinases in α-mangostin-induced apoptosis (Fig. 3), the profile of p-Erk1/2 levels indicated two peaks, one at the early phase (0.5–3 h) and the other at the late phase (24–48 h) of the treatment (Fig. 3). In contrast, the level of p-Akt increased at 0.5–1 h after the start of treatment and then drastically declined (Fig. 3). The level of p-p38 increased at 1–3 h of treatment. The level of p-JNK rose slightly and was sustained at this level after the start of treatment. Erk5 expression gradually decreased after the treatment (Fig. 3). It was earlier reported by us and others that microRNA-143 (miR-143) represses the expression of *ERK5* translationally.[8,9,11] Therefore, by semi-qRT-PCR we examined the expression levels of miR143 and *ERK5* mRNA. As shown in Figures 4a and b, the levels of miR-143 were significantly increased in a dose- and time-dependent manner by the treatment with α-mangostin which was confirmed by TaqMan® probe assay using real-time PCR. On the other hand, the level of *ERK5* mRNA evaluated by RT-PCR was almost unchanged (data not shown), suggesting that the miR-143 caused the decreased expression of the Erk5 protein at the translational level in α-mangostin-induced apoptosis. The level of *c-Myc*, whose transcription is regulated by a signal involving Erk5,[12,13] was also reduced concurrently with the down-regulation of Erk5 (Fig. 3).

### 2.4. Augmentation of growth suppression by co-treatment of DLD-1 cells with α-mangostin and 5-FU

The IC50 of 5-FU was 4.5 ± 0.4 μM for DLD-1 cells (Fig. 5a). We examined effects of the combined treatment of α-mangostin with 5-FU on cell growth. It should be noted that the growth suppressive activity toward DLD-1 cells by the combined treatment with these two agents, the concentrations of which were each half those used for the single agent, was higher than that achieved by the single treatment with α-mangostin or 5-FU at either 2 or 5 μM (Fig. 5a). These data indicate a synergistic effect of the combined treatment. However, above 5 μM, no significant synergistic effects were observed. In the case of the combined treatment with 2 or 5 μM (total), we did not observe any morphological changes indicative of apoptosis (Fig. 1c).

Next, we examined the effects of the combined treatment at a total of 5 μM on MAP kinases, Akt signaling, and cell cycle related proteins cyclin D1 and c-myc (Fig. 5b). The levels of p-Erk1/2 were increased at 6–12 h after the combined treatment with 5-FU and α-mangostin, which increase was similar to that obtain with the single treatment with 5 μM 5-FU or α-mangostin alone. The two phases of Erk1/2 activation induced by 20 μM α-mangostin (Fig. 3) were not observed after either the combined or single treatment. The level of Erk5, a target of miR-143, remained unchanged during the treatment (Fig. 5b).

The level of p-Akt gradually decreased with time of treatment with 5 μM α-mangostin; however, the level in response to 5 μM 5-FU increased up to 12 h and then decreased at 24 h. In the case of the combined treatment with 2.5 μM α-mangostin and 2.5 μM 5-FU, the levels of p-Akt were increased from 1 to 12 h and then considerably decreased at 24 h, which pattern was similar to that found for 5-FU alone.

We previously reported that the level of cyclin D1 was decreased in the early phase by treatment of DLD-1 cells with 20 μM α-mangostin treatment.[2] However, there were no significant change in the levels of cyclin D1 in these cells treated with 5 μM α-mangostin (Fig. 5b). In contrast, with 5 μM 5-FU treatment the level was consistently depressed. The expression profile for cyclin D1 after the combined treatment with each agent at 2.5 μM was similar to that obtained with the single treatment with 5 μM 5-FU; however, the reduction with the combined treatment was greater than that with the treatment with 5-FU alone. In addition, the profiles of c-Myc and cyclin D1 with these two treatments were very similar. In the combined treatment, the levels of

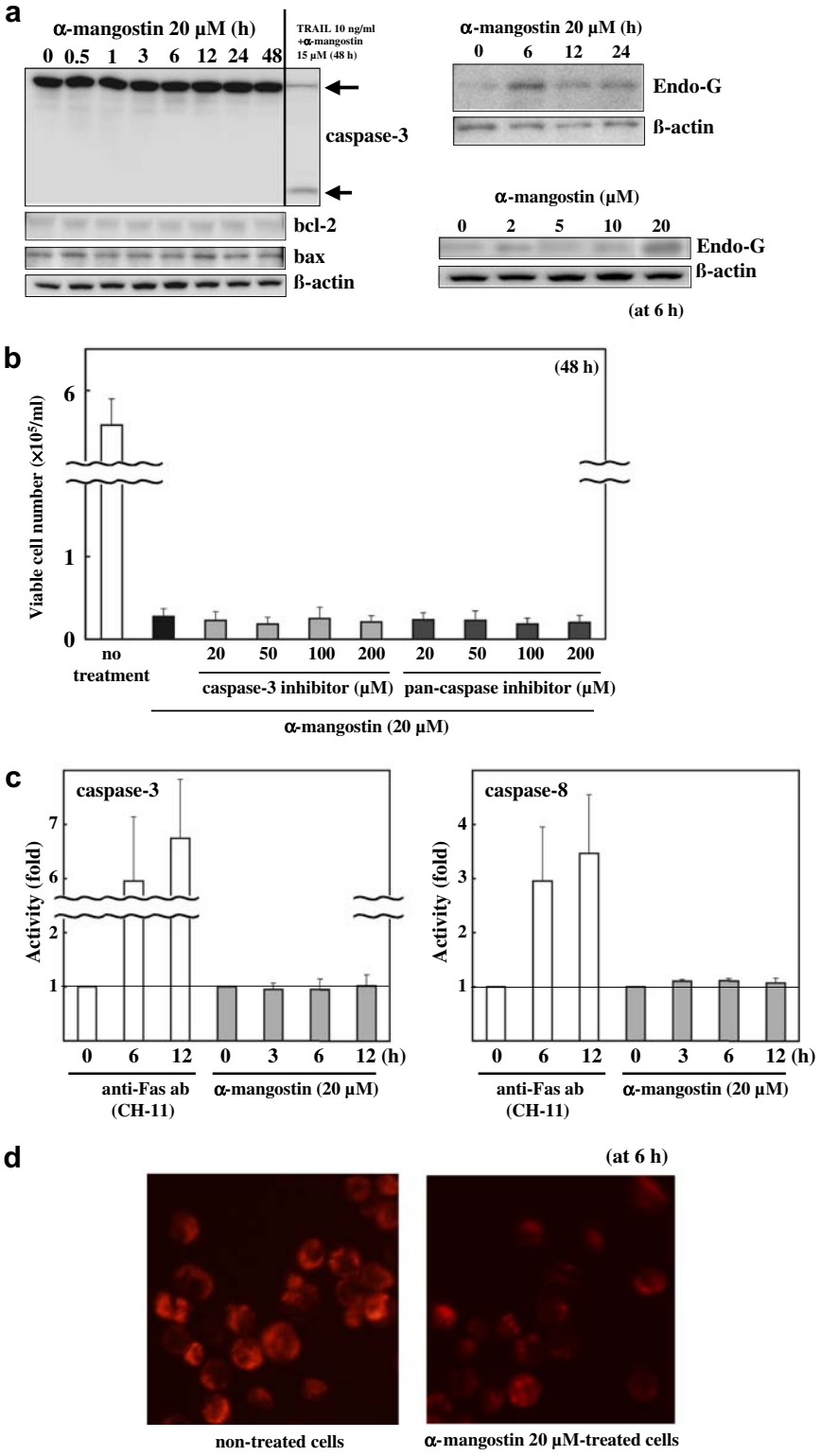


**Figure 2.** α-Mangostin-induced cell death in DLD-1 cells. (a) Lack of activation of caspase-3, bcl-2, and bax after treatment with 20 μM α-mangostin, as determined by Western blot analysis. Sample obtained from co-treatment with 10 ng/ml TRAIL and 15 μM α-mangostin in DLD-1 cells was used as a reference of caspase-3-dependent apoptosis. Release of Endo-G from mitochondria after treatment with 20 μM α-mangostin was examined by Western blot analysis. Western blots showing dose-dependent release of Endo-G after the treatment with α-mangostin for 6 h. (b) Effect of caspase-3 inhibitor Z-DEVD-FMK or pan-caspase inhibitor Z-VAD-FMK on 20 μM α-mangostin-induced apoptosis. The inhibitor was added 12 h before exposure to 20 μM α-mangostin. The rescue of cell death was evaluated at 48 h after the treatment with 20 μM α-mangostin in the presence of different concentrations of the inhibitor. (c) Activities of caspase-3 and -8 on 20 μM α-mangostin-induced apoptosis. Activities of them were measured colorimetrically with an assay kit. Anti-Fas antibody (CH-11) was used as reference of caspase-3 and -8 dependent apoptosis in Jurkat cells. (d) Mitochondrial membrane potential after 6-h treatment with 20 μM α-mangostin. Left, cells without treatment; right, treatment with 20 μM α-mangostin for 6 h.

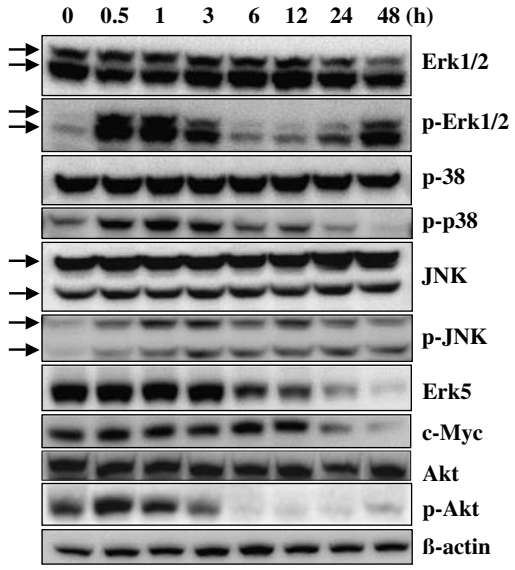


**Figure 3.** MAP kinases and Akt kinase in 20 μM α-mangostin-treated DLD-1 cells. Erk, p-Erk, p38, p-p38, JNK, p-JNK, Erk5, c-Myc, Akt, and p-Akt were examined by Western blot analysis.

c-Myc were transiently decreased at 1 h and then further reduced at 24 h, compared with the single 5 μM 5-FU treatment. The levels of miR-143 and miR-145 were not changed by either single or combined treatment (data not shown).

## 3. Discussion

The cytotoxic activity of α-mangostin has been shown to result from cell cycle arrest at G1/S and the subsequent apoptosis to be mediated by the intrinsic pathway in DLD-1 cells.[2] In this study, we intended to disclose the mechanism of α-mangostin-induced apoptosis in DLD-1 cells.[2] We previously reported that α-mangostin-induced apoptosis was mediated by the caspase-3 pathway in HL60 leukemia cells.[14] However, our present results with DLD-1 cells indicate that α-mangostin-induced apoptosis was mediated by a caspase-independent pathway via mitochondria with the release of Endo-G. During the last several years, it has become increasingly clear that mitochondria play a major rate-limiting role in apoptosis. The decision/effecter phase of the apoptotic process converges on mitochondria, where permeabilization of mitochondrial membranes is triggered, and apoptosis-inducing factors such as cytochrome c, AIF, and Endo-G are released. Endo-G, a known 30-kDa nuclease residing in mitochondria, is able to induce nucleosomal DNA fragmentation.[15] In our present study, we found that a large amount of Endo-G was released after 6 h of α-mangostin treatment. Accordingly, our data raise the possibility that Endo-G, and not caspases, may play a crucial role in DNA ladder formation in DLD-1 cells by some mechanism(s) that is not yet defined.[15]

The levels of p-p38 and p-JNK appeared to change within 24 h after the treatment with α-mangostin, but the significance of this change is not clear. The levels of p-Erk1/2 were increased in two separate phases by the treatment. Recently, it was reported that the expression profile of p-Erk1/2 showed also two peaks when HT-22 cells were exposed to glutamate-induced oxidative stress.[16] Erk1/2 may play dual roles, acting first as a cellular adaptive response during the initial phase and then as a cytotoxic response during the later stages of such stress. As reported,[16] the decline in p-Erk1/2 after the latter peak may be associated with the apoptotic machinery. As to Akt signaling, which is associated with cell survival, growth, and glycogen metabolism,[4] the level of p-Akt was markedly reduced at 6 h after the start of α-mangostin treatment (Fig. 3), which time is consistent with the occurrence of the apoptosis. Therefore, the level drops of Akt signaling could participate in the mechanism of apoptosis induced by α-mangostin.

Erk5 is known to promote cell growth and proliferation.[17] And c-myc, which is an oncoprotein for the cell cycle, lies downstream in the cell growth signaling pathway including Erk5.[12,13] The microRNAs are an extensive class of small noncoding RNAs, 18–24 nucleotides in length, with the role of regulating gene expression through translational repression by base-pairing with partially complementary mRNAs.[18] The translational

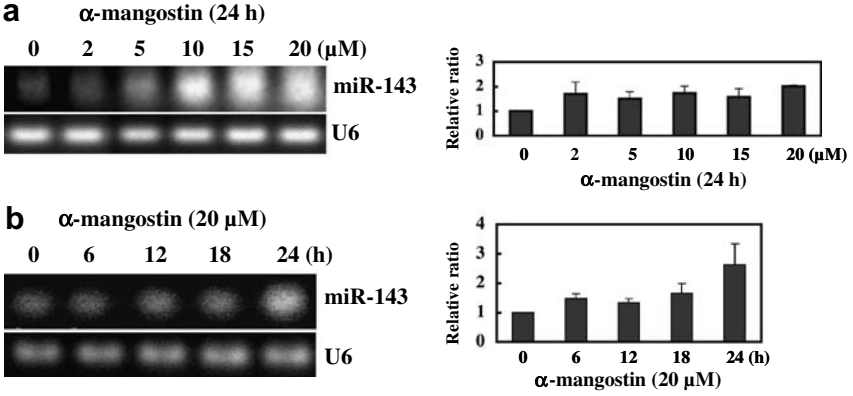


**Figure 4.** Semi-qRT-PCR-evaluated or TaqMan® probe assay (real-time PCR)-evaluated miRNA-143. (a) Expression levels of miR-143 in DLD-1 cells treated with various concentrations of α-mangostin for 24 h. (b) The expression levels of miR-143 at various times during treatment of the cells with 20 μM α-mangostin. At real-time PCR, the relative value of nontreated DLD-1 cells was designated as 1.

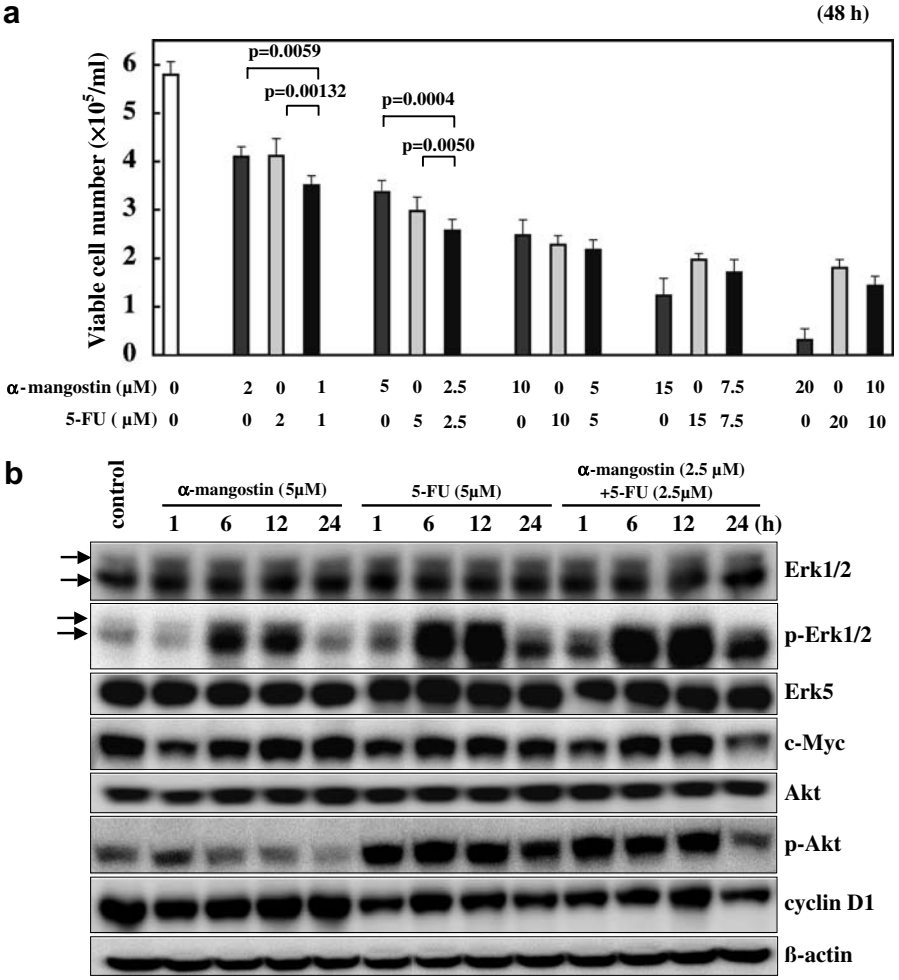


**Figure 5.** Synergistic growth-inhibiting effect by the combined treatment of DLD-1 cells with α-mangostin and 5-FU. (a) Growth suppression due to combined treatment with α-mangostin and 5-FU at equally 2.5 μM or to the single treatment with each agent. Concentrations tested are shown on the abscissa. Cell numbers after treatment with α-mangostin were evaluated by use of the Trypan blue dye-exclusion test. (b) Expression profiles of MAP kinases, Akt kinase, and cell cycle related c-Myc, and cyclin D1 during the treatment with α-mangostin and/or 5-FU in DLD-1 cells. Erk, p-Erk, Erk5, c-Myc, Akt, p-Akt, and cyclin D1 were examined by Western blot analysis.

repression of *ERK5* mRNA was earlier shown to be exerted by miR-143.[8,9,11] In α-mangostin-induced apoptosis of DLD-1 cells, the levels of Erk5 and c-myc protein gradually decreased during the period of α-mangostin treatment. The levels of miR-143 were significantly increased, whereas the levels of *ERK5* mRNAs were almost unchanged, suggesting that α-mangostin may have elevated the expression of miR-143 probably by modulating its transcription and/or the upstream signals associated with the transcription factors of miR-143.[19]

5-FU is one of the most effective chemotherapeutic agents for colorectal adenocarcinoma.[20] 5-FU can produce response rates of ~11% when used as a single agent.[19] Strategies aimed at enhancing the therapeutic efficiency of 5-FU and decreasing the side effect have involved its administration schedule and also its use in combination with other anti-cancer or biochemical-modulating agents to produce a better treatment response.[21] For example, folinic acid,[19] leucovorin (LV),[21,22] oxaliplatin (L-OHP), LV in the FOLFOX regimen,[23] and irinotecan (CPT-11) and LV in the FOLFIRI regimen[24] are combination therapies for colorectal cancer patients. In view of recent phytochemical studies, it has been expected that such substances included in vegetables and fruits could affect the efficacy of anti-cancer drugs and their metabolism.[25] Therefore, it is very important for us to study the interaction between phytochemicals and anti-cancer drugs. In the current study, we demonstrated the synergistic effect on cell growth when 5-FU was combined with the phytochemical α-mangostin used at low concentrations such that the total for both agents was 2 or 5 μM (Fig. 5a). The growth inhibition by 5-FU was probably due to cell cycle arrest at the concentrations tested,[26] because no apoptotic cells were observed. At more than 15 μM α-mangostin, apoptotic cells were observed; whereas at lower concentrations α-mangostin most likely exerts cell cycle arrest[2] like 5-FU. Thus, the synergistic effect by the combined treatment at the total 2 and 5 μM concentrations was probably due to the additional enhancement of machinery leading to cell cycle

arrest. Indeed, the expression of cell cycle related proteins such as cyclin D and c-myc at total 5 μM was significantly reduced at 24 h, compared with that found for each agent alone (Fig. 5b).

It is possible that the mechanism of growth suppression by α-mangostin is different from that of 5-FU at more than 15 μM, because the growth inhibition obtained by a single treatment with α-mangostin was greater than that when the combined treatment was used. Possibly, the more potent apoptosis-inducing activity of α-mangostin, which was observed at more than 15 μM, was not induced by the combination with 5-FU at both 7.5 and 10 μM. In this context, the activation of MAP kinases and Akt signal pathways, which were shown to be changed by the treatment with 20 μM α-mangostin alone, may also be weakened in the single treatment of α-mangostin or 5-FU. Thus, phytochemicals could have a considerable effect on the efficacy of anti-cancer agents, depending on their concentrations, by affecting intracellular signal transduction.[21,25]

We previously reported that α-mangostin had potent chemopreventive effects in a short-term rat colon carcinogenesis bioassay and also that it did not show acute or semi-acute toxicity.[27] The findings presented here indicate that α-mangostin modulated MAP kinases and Akt signaling, leading to apoptotic cell death and also that it exhibited a synergistic effect on 5-FU-induced growth inhibition at the lower concentrations. Therefore, with α-mangostin it may be possible to reduce the dose of 5-FU in clinical use. However, further studies will be needed to elucidate how α-mangostin negatively regulates the growth of cancer cells in vitro and in vivo.

## 4. Conclusion

The present study showed that the cytotoxic effect of 20 μM α-mangostin was found to be mainly due to apoptosis which was found to be caspase-independent. However, endonuclease-G released from mitochondria with the decreased mitochondrial membrane potential was shown. At the same time, the level of phospho-Akt was sharply reduced with the process of apoptosis after 6 h of treatment. Interestingly, the level of microRNA-143, which negatively regulates Erk5 at translation, gradually increased until 24 h following the start of treatment. We also demonstrated that α-mangostin acts as an effective chemosensitizer at a certain concentration. These results indicate that α-mangostin could be one of candidate compounds for chemopreventive and therapeutic agent for cancers.

## 5. Experimental

### 5.1. Agents

α-Mangostin was purified to greater than 98% as described in our previous studies.[1,2] 5-FU, a commonly used anti-cancer drug for the treatment of colorectal adenocarcinoma, was purchased from a commercial source (Sigma–Aldrich Co., MO). Both were dissolved in DMSO at the concentration of 20 mM and further diluted to the desired working concentration before use.

### 5.2. Cell culture, morphological study, and cell viability

Human colon cancer DLD-1 cells were grown in RPMI-1640 medium supplemented with 10% (v/v) heat-inactivated fetal bovine serum (Sigma, Tokyo) and 2 mM L-glutamine under an atmosphere of 95% air and 5% $CO_2$ at 37 °C. Cell viability was determined by used of the Trypan blue dye-exclusion assay. For morphological examination of apoptotic changes, cells were stained with Hoechst 33342 (5 μg/ml) at 37 °C for 30 min, washed twice with phosphate-buffered saline (PBS), pipetted dropwise onto a glass slide, and examined by fluorescence microscopy using an Olympus microscope (Tokyo, Japan) equipped with an epi-illuminator and appropriate filters. Co-treatment or single treatment of the cells with 5-FU and/or α-mangostin was started at 16 h after the cells had been plated at the concentration of $1 \times 10^5$ cells/ml.

### 5.3. Western blot analysis

Before and after treatment with α-mangostin, DLD-1 cells were washed twice with PBS, lysed in lysis buffer A or B, and then homogenized. Cells were lysed with lysis buffer A (250 mM sucrose, 20 mM Hepes–KOH (pH 7.5), 10 mM KCl, 1.5 mM $MgCl_2$, 1 mM EDTA, 1 mM EGTA, 1 mM DTT, and 25 × Complete®) to analyze AIF and endonuclease-G. For analysis of other proteins, lysis buffer B (2 × PBS, 0.1% SDS, 1% Nonidet P-40, 0.5% sodium deoxycholate, and 25 × Complete®, a mixture of protease inhibitors (Roche, Penzberg Germany)®, and Phosphatase Inhibitor Cocktail® 1 and 2 (Sigma–Aldrich Co.)) was used. The mitochondrial and cytosolic fractions were prepared as reported previously.[8] A suitable amount of protein of each cell lysate was separated by SDS–PAGE by using a 7.5%, 10%, or 12.5% polyacrylamide gel and the separated proteins were then electroblotted onto a PVDF membrane (Du Pont, Boston, MA). After blockage of nonspecific binding sites for 1 h by 5% nonfat milk in TPBS (PBS and 0.1% Tween 20), the membrane was incubated overnight at 4 °C with various antibodies. They included anti-human caspase-3 (Santa Cruz Biotechnology, CA), anti-human caspase-8 (MBL, Nagoya, Japan), anti-human bcl-2 (Santa Cruz Biotechnology), anti-human bax (Santa Cruz Biotechnology), anti-human AIF (ProSci Inc., CA), anti-human endonuclease-G (Endo-G; Sigma–Aldrich Co.), anti-human p44/42 MAP Kinase (Erk1/2; Cell Signaling Technology Inc., MA), anti-human phospho-p44/42 MAPK (Thr202/Tyr204, p-Erk1/2; Cell Signaling Technology Inc.), anti-human p38 MAP kinase (p38, Cell Signaling Technology Inc.), anti-human phospho-p38 MAP kinase (Thr180/Tyr182, p-p38; Cell Signaling Technology Inc.), anti-human SAPK/JNK (JNK, Cell Signaling Technology Inc.), anti-human phospho-SAPK/JNK (Thr183/Tyr185, p-JNK; Cell Signaling Technology

Inc.), anti-human Erk5 (Cell Signaling Technology Inc.), anti-human c-Myc (Santa Cruz Biotechnology), anti-human Akt (Cell Signaling Technology Inc., MA), anti-human phospho-Akt (Ser473, p-Akt; Cell Signaling Technology Inc.), anti-human Cyclin D1 (Cell Signaling Technology Inc.), and anti-human β-actin (Sigma–Aldrich Co.). Each electroblotted membrane was then washed three times with TPBS, incubated further with alkaline phosphatase-conjugated goat anti-mouse antibody (Promega, Madison, WI) or anti-rabbit antibody (New England Biolabs, Beverly, MA) at room temperature, and then washed three times with TPBS. The immunoblot was visualized by use of an enhanced chemiluminescence detection kit (New England Biolabs).

### 5.4. Inhibition of apoptosis by caspase inhibitors

For the study of inhibition of apoptosis, the tripeptide caspase-3 inhibitor Z-DEVD-FMK (MBL) or pan-caspase inhibitor Z-VAD-FMK (MBL) was added to the culture medium 12 h before treatment with α-mangostin. The optimal concentration of the inhibitor was determined from a dose–response curve for the extent of cell death. Each caspase inhibitor was used at the concentrations of 20–200 μM. Inhibition of apoptosis by the inhibitors was evaluated by cell number which was determined by the Trypan blue dye-exclusion assay and Hoechst 33342 nuclear staining.

### 5.5. Caspase activity assay

Activities of caspase-3 and -8 were measured colorimetrically with a commercial assay kit (Alexis Biochemicals, Lausen, Switzerland). Briefly, the cells treated or not with 20 μM α-mangostin were washed twice in ice-cold PBS, and cell lysates were prepared according to the manufacturer's instructions. Cell lysates containing 100 μg of protein were incubated with pNA-conjugated substrate, and the release of pNA was measured at 405 nm by using a microplate reader NJ-2300 (NUNC, Rockilde, Denmark).

### 5.6. Measurement of mitochondrial membrane potential using Mito-Traker probe

Mitochondrial membrane potential was measured by use of a fluorescent dye, Mito-Tracker Orange (Molecular Probes, #M-7511, Eugene, OR), which accumulates selectively in active mitochondria and becomes fluorescent when oxidized. After the cells were treated with Mito-Tracker Orange solution and washed twice with PBS, the cells were resuspended in PBS. The fluorescence of Mito-Tracker Orange in the cells was observed under fluorescence microscope (Olympus).

### 5.7. Semi-quantitative RT-PCR

Before and after treatment with α-mangostin, DLD-1 cells were washed twice with PBS. RT-PCR was performed as described previously.[28] In brief, total RNA was isolated from the cells and tissues by the phenol/guanidium thiocyanate method with DNase I treatment. To determine the expression of miRNAs, we measured their levels by using a mirVanaTM qRT-PCR miRNA Detection Kit (Ambion) and mirVanaTM qRT-PCR Primer set (Ambion). Briefly, after reverse transcription of 50 ng of total RNA, cDNA was generated. The PCR consisted of 22 cycles (95 °C for 15 s, 60 °C for 30 s) after an initial denaturation step (95 °C for 3 min). U6 (RUN6B) was used as an internal control. The PCR primer pairs for miR-143 were obtained commercially from Ambion. The PCR products were confirmed to be miRNA loci of miR-143 by DNA sequencing.

To determine the levels of mRNAs, cDNA samples were purified by use of a PCR Purification kit (Qiagen, Hilden, Germany) and used for PCR (Takara, Ohtsu, Japan). The primers for ERK5 were as follows: ERK5-sense-211, 5′-CCTTCGATGTGACCTTTGAC-3′; ERK5-antisense-1418, 5′-TGACACCATTGATCT GACCC-3′. The PCR consisted of 30 cycles (94 °C for 30 s, 57.5 °C for 1 min, 72 °C for 1 min) after an initial denaturation step (95 °C for 1 min). The PCR products were analyzed by electrophoresis on 2% agarose gels.

### 5.8. Real-time PCR

cDNA was synthesized from total RNA using gene-specific primers according to the protocol of TaqMan® MicroRNA Assays (Applied Biosystems, Foster City, CA).[29] Reverse transcriptase reactions contained 10 ng of RNA samples, 50 nM stem and loop RT primer (TaqMan® MicroRNA Assays; Applied Biosystems), and reagents of TaqMan® MicroRNA Reverse Transcription Kit (Applied Biosystems). The 15 μl reaction mixtures were incubated for 30 min at 16 °C, 30 min at 42 °C, 5 min at 85 °C and then held at 4 °C. Real-time PCR was performed using a PCR primer (TaqMan® MicroRNA Assays; Applied Biosystems) and reagent of LightCycler® TaqMan® Master (Roche Diagnostics, Mannheim Germany) on a LightCycler (Software Version 3.5, Roche). The 20 μl PCRs included 1.33 μl RT-PCR product, 4 μl reagent of LightCycler® TaqMan® Master (Roche Diagnostics), and 1 μl PCR primer (TaqMan® MicroRNA Assays; Applied Biosystems). These reaction mixtures were incubated at 95 °C for 10 min, followed by 50 cycles of 95 °C for 10 s, 60 °C for 40 s, and 72 °C for 1 s. All reactions were run in duplicate. The threshold cycle ($C_T$) is defined as the fractional cycle number at which the fluorescence passes the fixed threshold. miR-143 and miR145 levels in each cells were measured and were normalized to U6 which was used as an internal control. The relative value of nontreated DLD-1 cells was designated as 1.

## Acknowledgment

This work was supported in part by a grant from the program Grant-in-Aid for Young Scientists (B) of the Japan Society for the Promotion of Science.

## References and notes


1. Matsumoto, K.; Akao, Y.; Kobayashi, E.; Ohguchi, K.; Itou, T.; Tanaka, T.; Iinuma, M.; Nozawa, Y. *J. Nat. Prod.* **2003**, *66*, 1124–1127.
2. Matsumoto, K.; Akao, Y.; Ohguchi, K.; Itou, T.; Tanaka, T.; Iinuma, M.; Nozawa, Y. *Bioorg. Med. Chem.* **2005**, *13*, 6064–6069.
3. Roux, P. P.; Blenis, J. *Microbiol. Mol. Biol. Rev.* **2004**, *68*, 320–344.
4. Pap, M.; Cooper, G. M. *J. Biol. Chem.* **1998**, *273*, 19929–19932.
5. Sah, J. F.; Balasubramanian, S.; Eckert, R. L.; Rorke, E. A. *J. Biol. Chem.* **2004**, *279*, 12755–12762.
6. Aggarwal, B. B.; Bhardwaj, A.; Aggarwal, R. S.; Seeram, N. P.; Shishodia, S.; Takada, Y. *Anticancer Res.* **2004**, *24*, 2783–2840.
7. Nakagawa, Y.; Iinuma, M.; Matsuura, N.; Yi, K.; Naoi, M.; Nakayama, T.; Nozawa, Y.; Akao, Y. *J. Pharmacol. Sci.* **2005**, *97*, 242–252.
8. Akao, Y.; Nakagawa, N.; Naoe, T. *Oncol. Rep.* **2006**, *16*, 845–850.
9. Akao, Y.; Nakagawa, Y.; Naoe, T. *DNA Cell Biol.* **2007**, *26*, 311–320.
10. Tsujimoto, Y.; Shimizu, S. *FEBS Lett.* **2000**, *466*, 6–10.
11. Esau, C.; Kang, X.; Peralta, E.; Hanson, E.; Marcusson, E. G.; Ravichandran, L. V.; Sun, Y.; Koo, S.; Perera, R. J.; Jain, R.; Dean, N. M.; Freier, S. M.; Bennett, C. F.; Lollo, B.; Griffey, R. *J. Biol. Chem.* **2004**, *279*, 52361–52365.
12. Sharma-Walia, N.; Krishnan, H. H.; Naranatt, P. P.; Zeng, L.; Smith, M. S.; Chandran, B. *J. Virol.* **2005**, *79*, 10308–10329.
13. English, J. M.; Pearson, G.; Baer, R.; Cobb, M. H. *J. Biol. Chem.* **1998**, *273*, 3854–3860.
14. Matsumoto, K.; Akao, Y.; Yi, H.; Ohguchi, K.; Ito, T.; Tanaka, T.; Kobayashi, E.; Iinuma, M.; Nozawa, Y. *Bioorg. Med. Chem.* **2004**, *15*, 5799–5806.
15. Li, L. Y.; Luo, X.; Wang, X. *Nature* **2001**, *412*, 95–99.
16. Luo, Y.; DeFranco, D. B. *J. Biol. Chem.* **2006**, *281*, 16436–16442.
17. Nishimoto, S.; Nishida, E. *EMBO Rep.* **2006**, *7*, 782–786.
18. Ambros, V. *Cell* **2003**, *113*, 673–676.
19. Wein, A.; Riedel, C.; Bruckl, W.; Kastl, S.; Reingruber, B.; Hohenberger, W.; Hahn, E. G. *Gastroenterology* **2001**, *39*, 153–156.
20. Tai, C. J.; Liu, J. H.; Chen, W. S.; Lin, J. K.; Wang, W. S.; Yen, C. C.; Chiou, T. J.; Chen, P. M. *Jpn. J. Clin. Oncol.* **2003**, *33*, 136–140.
21. Zalcberg, J.; Kerr, D.; Seymour, L.; Palmer, M. *Eur. J. Cancer* **1998**, *34*, 1871–1875.
22. Petrelli, N.; Douglass, H. O., Jr.; Herrera, L.; Russell, D.; Stablein, D. M.; Bruckner, H. W.; Mayer, R. J.; Schinella, R.; Green, M. D.; Muggia, F. M. *J. Clin. Oncol.* **1989**, *7*, 1419–1426.
23. Maindrault-Goebel, F.; de Gramont, A.; Louvet, C.; Andre, T.; Carola, E.; Mabro, M.; Artru, P.; Gilles, V.; Lotz, J. P.; Izrael, V.; Krulik, M. *Eur. J. Cancer* **2001**, *37*, 1000–1005.
24. Mabro, M.; Artru, P.; Andre, T.; Flesch, M.; Maindrault-Goebel, F.; Landi, B.; Lledo, G.; Plantade, A.; Louvet, C.; de Gramont, A. *Br. J. Cancer* **2006**, *94*, 1287–1292.
25. Bava, S. V.; Puliappadamba, V. T.; Deepti, A.; Nair, A.; Karunagaran, D.; Anto, R. J. *J. Biol. Chem.* **2005**, *280*, 6301–6308.
26. Kawashima, R.; Haisa, M.; Kimura, M.; Takaoka, M.; Shirakawa, Y.; Takeda, H.; Uetsuka, H.; Gunduz, M.; Nagai, N.; Tanaka, N.; Naomoto, Y. *Int. J. Oncol.* **2004**, *24*, 273–278.
27. Nabandith, V.; Suzui, M.; Morioka, T.; Kaneshiro, T.; Kinjo, T.; Matsumoto, K.; Akao, Y.; Iinuma, M.; Yoshimi, N. *Asian Pac. J. Cancer Prev.* **2004**, *5*, 433–438.
28. Akao, Y.; Otsuki, Y.; Kataoka, S.; Ito, Y.; Tsujimoto, Y. *Cancer Res.* **1994**, *54*, 2468–2471.
29. Chen, C.; Ridzon, D. A.; Broomer, A. J.; Zhou, Z.; Lee, D. H.; Nguyen, J. T.; Barbisin, M.; Xu, N. L.; Mahuvakar, V. R.; Andersen, M. R.; Lao, K. Q.; Livak, K. J.; Guegler, K. J. *Nucleic Acids Res.* **2005**, *33*, e179.